PERGAMON

International Journal of Solids and Structures 40 (2003) 3253–3271

INTERNATIONAL JOURNAL OF SOLIDS and STRUCTURES

www.elsevier.com/locate/ijsolstr

A self-stabilized algorithm for enforcing constraints in multibody systems

Olivier A. Bauchau

School of Aerospace Engineering, Georgia Institute of Technology, 270 Ferst Drive, Atlanta, GA 30332-0150, USA

Received 28 September 2002; received in revised form 13 February 2003

Abstract

A new algorithm is developed for the enforcement of constraints within the framework of nonlinear, flexible multibody system modeled with the finite element approach. The proposed algorithm exactly satisfies the constraints at the displacement and velocity levels, and furthermore, it achieves nonlinear unconditional stability by imposing the vanishing of the work done by the constraint forces when combined with specific discretizations of the inertial and elastic forces. Identical convergence rates are observed for the displacements, velocities, and Lagrange multipliers. The proposed algorithm is closely related to the stabilized index-2 or GGL method, although no additional multipliers are introduced in the present approach. These desirable characteristics are obtained without resorting to numerically dissipative algorithms. If high frequencies are present in the system, i.e. the system is physically stiff, dissipative schemes become necessary; the proposed algorithm is extended to deal with this situation.

Keywords: Multibody dynamics; Nonlinear constraints; Constraint stabilization

1. Introduction

Multibody dynamics analysis was originally developed as a tool for modeling mechanisms with simple tree-like topologies composed of rigid bodies, but has considerably evolved to the point where it can handle nonlinear flexible systems with arbitrary topologies (Nikravesh, 1988; Amirouche, 1992). Multibody systems can be viewed as a collection of rigid or flexible bodies connected by joints that impose constraints on the relative motion of the various bodies of the system. The unavoidable presence of these joints is a distinguishing feature of multibody systems. Most joints used for practical applications can be modeled in terms of the so called *lower pairs* (Angeles, 1982): the revolute, prismatic, screw, cylindrical, planar and spherical joints. In many cases however, joints with specialized kinematic conditions must be developed. Although it is possible to work with a minimum set of coordinates to represent the system, it is often more convenient to use a redundant set subjected to constraints. Typically, the constraints are then enforced via

E-mail address: oliver.bauchau@ae.gatech.edu (O.A. Bauchau).

0020-7683/03/$ - see front matter © 2003 Elsevier Science Ltd. All rights reserved.
doi:10.1016/S0020-7683(03)00159-8

the Lagrange multiplier technique, and the resulting equations of motion then form a set of differential-algebraic equations (DAEs). A good review of the many methods that have been developed for dealing with constrained multibody systems can be found in (Schiehlen, 1990). Four broad classes of method will be reviewed in the following paragraphs.

A first approach to the analysis of constrained multibody systems is to eliminate the redundant degrees of freedom and work with a minimum set. Typically, the equations of motion are projected onto the tangent to the constraint manifold to determine the independent and dependent degrees of freedom. Many techniques find their basis in this decomposition approach: the zero eigenvalue method (Walton and Steeves, 1969), the coordinate partitioning method (LU factorization; Wehage and Haug, 1982), the singular decomposition method (Singh and Likins, 1985; Mani et al., 1985), the QR or householder decomposition (Kim and Vanderploeg, 1986; Amirouche et al., 1988), and the Gramm–Schmidt orthogonalization (Liang and Lance, 1987; Agrawal and Saigal, 1989). It has been shown by Kurdila et al. (1990) and Papastavridis (1990) that all of these methods can be unified within the framework of Maggi's equation. Unfortunately, these methods are not a practical approach when dealing with finite element formulations because they destroy the banded nature of the governing equations.

Another approach is to work with the original set of DAEs. Gear and Petzold (1984), Lotstedt and Petzold (1986a,b) and Brenan et al. (1989) have given a formal definition of the index of a system of DAEs. The governing equations for mechanical systems with holonomic constraints are index-3 DAEs; typically, higher indices result in more arduous solution processes. Gear et al. (1985) proposed a method, called the stabilized index-2 or GGL method, that reduces the index from 3 to 2 and showed that variable-order, variable-step backward difference methods converge for the resulting index-2 problem. Later, Gear (1988) developed an approach to further reduce the problem to index-1 DAEs. Of course, these approaches require additional computational cost in the form of additional Lagrange multipliers. Another approach to index reduction is the embedded projection method (Borri et al., in press) that can be used to systematically reduce the index from 3 to 1. Furthermore, it splits the original DAE problem into its algebraic and differential parts.

The third approach also involves index reduction techniques, as should be expected in view of the numerical difficulties associated with index-3 DAEs. However, in this case, index reduction is achieved by enforcing a time derivative of the constraint. Let $\mathscr{C} = 0$, $\dot{\mathscr{C}} = 0$ and $\ddot{\mathscr{C}} = 0$ represent the displacement, velocity and acceleration level constraints, respectively. The system formed by the equations of motion and the acceleration level constraints then forms a set of index-1 DEAs with invariants. Indeed, for the exact solution, $\mathscr{C} = 0$ and $\dot{\mathscr{C}} = 0$ represent two invariants of the system. Unfortunately, an approximate numerical solution will not evolve on the invariant manifolds, resulting in $\mathscr{C} \neq 0$ and $\dot{\mathscr{C}} \neq 0$. Baumgarte's stabilization method (Baumgarte, 1972) was introduced to compensate for this drift. However, this approach never exactly satisfies the constraints, and relies on problem dependent parameters for adequate performance. Park and Chiou (1988) and Park et al. (1988) presented a procedure that achieves stabilization based on a penalty form of the constraint equations. Finally, Bayo et al. (1988) and Bayo and Ledesma (1996) proposed an augmented Lagrangian approach and a mass-orthogonal projection was used to satisfy the displacement, velocity, and acceleration level constraints to machine accuracy.

The last set of methods attacks the index-3 DAEs without *prior index reduction*. Orlandea et al. (1977) used numerically dissipative time integrators specifically designed for stiff problems to directly integrate these equations. Within the framework of finite element formulations for multibody dynamics (Géradin and Cardona, 2000), the governing equations of motion form a large set of sparse equations for the displacement variables and Lagrange multipliers, i.e. a set of index-3 DAEs. Cardona and Géradin (1989) showed that the classical Newmark (1959) trapezoidal rule is unconditionally unstable for linear systems in the presence of constraints. However, the use of dissipative algorithms such as HHT (Hilber et al., 1977)

resulted stable behavior, even for nonlinear systems. Further work by Farhat et al. shows that both HHT and generalized-α (Chung and Hulbert, 1993) methods achieve stability for a class of constrained hybrid formulations. In these approaches, stabilization of the integration process is inherently associated with the dissipative nature of the algorithms.

In recent years, considerable work has been done with energy preserving (EP) schemes and energy decaying (ED) schemes. Whereas the classical schemes (Newmark, HHT, or generalized-α) used in finite element procedures come with proofs of unconditional stability for linear systems, EP and ED schemes feature unconditional nonlinear stability. For EP schemes, discretizations of the inertial and elastic forces in rigid bodies (Simo and Wong, 1991; Simo and Tarnow, 1992), beams (Bauchau et al., 1995; Simo et al., 1995), plates, and shells (Simo and Tarnow, 1994) have been developed that preserve the total mechanical energy of the system at the discrete solution level. In view of the positive definite nature of the total mechanical energy, this discrete conservation law guarantees the stability of the computational scheme for nonlinear problems. Puso (2002) developed an energy conserving scheme for rigid–flexible body dynamics with constraints between the rigid bodies; this scheme achieves nonlinear unconditional stability for a specific type of constraint. However, while nonlinear unconditional stability is the first step towards the development of robust algorithms, it does not guarantee, per se, satisfactory performance of the scheme (Bauchau et al., 2003).

For nonlinear flexible multibody systems, EP schemes perform rather poorly when applied to complex simulations of engineering interest (Bauchau et al., 1995). The time histories of internal forces and velocities often present a very significant high frequency content that will hinder the solution convergence process. Furthermore, this high frequency response is an artifact of the spatial discretization process and contains no information about the physical behavior of the system. Hence, the presence of high frequency numerical dissipation is an indispensable feature of robust time integrators for multibody systems. This prompted the development of ED schemes for beam (Bottasso and Borri, 1997; Bauchau, 1998), shells (Bauchau et al., 2002) and multibody systems (Bottasso et al., 2001a,b).

In present work, a new algorithm is developed for the enforcement of constraints within the framework of nonlinear, flexible multibody system modeled with the finite element approach (Géradin and Cardona, 2000), where constraints are typically enforced through the Lagrange multiplier technique. The stiffness of the resulting equations stems from two sources: the "infinite" frequencies associated with the massless Lagrange multipliers, and the very high frequencies associated with the elastic components (beam, plates, or shells) of the system. It must be noted that the former stiffness is due to the formulation: Lagrange multiplier could be, in principle, eliminated by using a minimum set of coordinates, whereas the latter is inherent to the physical nature of the system. The proposed algorithm exactly satisfies the constraints at the displacement and velocity levels, and furthermore, it achieves nonlinear unconditional stability by imposing the vanishing of the work done by the constraint forces. The algorithm is second order accurate for displacements, velocities, and Lagrange multipliers. It is also shown that the proposed algorithm is closely related to the stabilized index-2 or GGL method (Gear et al., 1985), although no additional unknowns are introduced in the present approach. These desirable characteristics are obtained without resorting to numerically dissipative algorithms. Since the "infinite" frequencies associated with the Lagrange multipliers are indeed an artifact of the formulation rather than a physical characteristic of the system, it does not seem appropriate to use dissipative algorithms to solve the numerical problems resulting from enforcement of the constraints. If high frequencies are present, i.e. the system is physically stiff, ED schemes become necessary; the proposed algorithm will be extended to deal with this situation.

Section 2 defines the notation used to describe constrained dynamical problems. The EP version of the proposed algorithm is introduced in Section 3 for scleronomic, rheonomic, and non-holonomic constraints, and its ED version is then presented in Section 4. The relationship of the proposed algorithm with the GGL method is discussed in Section 5, and finally, numerical examples are presented in Section 6.

2. Constrained dynamical problems and notations

The semi discrete equations of motion for constrained multibody problems are written in a generic manner as

$$\underline{\mathscr{F}}^{\mathrm{I}}(\underline{u},\dot{\underline{u}},\ddot{\underline{u}})+\underline{\mathscr{F}}^{\mathrm{E}}(\underline{u})+B(\underline{u},t)\underline{\lambda}=\underline{\mathscr{F}}^{\mathrm{A}}, \tag{1}$$

where the three terms on the left hand side represents the inertial, elastic, constraint forces, respectively, whereas the externally applied loads appear on the right hand side. Array $\underline{u}$ stores the degrees of freedom of the system, $\underline{\lambda}$ is the array of Lagrange multipliers, B the constraint Jacobian matrix, and t denotes time. For Lagrangian systems, the inertial and elastic forces can be derived from the kinetic and strain energy functions, denoted $\mathscr{K}(\underline{u},\dot{\underline{u}})$ and $\mathscr{V}(\underline{u})$, respectively. It will be assumed that, in the absence of externally applied loads, the system is conservative; this implies the conservation of the total mechanical energy of the system, i.e. $\mathscr{E}=\mathscr{K}+\mathscr{V}$ is an invariant of the system. The constraint forces result from the enforcement of m constraint conditions via the Lagrange multiplier technique. Non-holonomic constraints are assumed to be linear with respect to velocities and are written in the following form

$$B^{\mathrm{T}}(\underline{u},t)\dot{\underline{u}}+\underline{a}(\underline{u},t)=0, \tag{2}$$

where the constraint Jacobian matrix is of rank m in order to avoid redundant constraints on the system. If these equations can be integrated to the form $\underline{\mathscr{C}}(\underline{u},t)=0$, the constraints are said to be holonomic and

$$\underline{\mathscr{C}}(\underline{u},t)=0. \tag{3}$$

In this case, the system must evolve on the constraint manifold, i.e. $\underline{\mathscr{C}}(\underline{u},t)=0$ is an invariant of the system, and $\dot{\underline{\mathscr{C}}}=0$, $\ddot{\underline{\mathscr{C}}}=0$, etc. clearly are additional invariants. In the presence of holonomic constraints, the equations of motion consist of Eqs. (1) and (3) and form a system of index-3 DAEs (Gear and Petzold, 1984). For non-holonomic constraints Eqs. (1) and (2) form a system of index-2 DAEs. Of course, both holonomic and non-holonomic constraints could appear simultaneously, resulting in a system of index-3 DAEs.

3. Proposed algorithm

The proposed self-stabilized method starts with the following discretization of the equations of motion, Eq. (1), at the mid-point of a typical time step

$$\underline{\mathscr{F}}^{\mathrm{I}}_{\mathrm{m}}+\underline{\mathscr{F}}^{\mathrm{E}}_{\mathrm{m}}+B_{\mathrm{m}}\underline{\lambda}_{\mathrm{m}}=\underline{\mathscr{F}}^{\mathrm{A}}_{\mathrm{m}}. \tag{4}$$

The velocity-displacement relationship are approximated as

$$\frac{\underline{u}_{\mathrm{f}}-\underline{u}_{\mathrm{i}}}{\Delta t}=\frac{\underline{v}_{\mathrm{f}}+\underline{v}_{\mathrm{i}}}{2}, \tag{5}$$

where $\underline{v}=\dot{\underline{u}}$ is the velocity array. The initial and final times for the time step are denoted t_{i} and t_{f}, respectively, and subscripts $(\cdot)_{\mathrm{i}}$ and $(\cdot)_{\mathrm{f}}$ will be used to indicate the value of a specific quantity at times t_{i} and t_{f}, respectively; $\Delta t=t_{\mathrm{f}}-t_{\mathrm{i}}$. The subscript $(\cdot)_{\mathrm{m}}$ indicates the "mid-point value" of the corresponding quantity. At the heart of the proposed algorithm is the selection of these mid-point values that will be guided by the requirement of preservation of system invariants.

For simplicity of the exposition, the case of holonomic constraints will be treated first, and furthermore, constraints will be assumed to be scleronomic, i.e. $\underline{\mathscr{C}}=\underline{\mathscr{C}}(\underline{u})$. Next, the case rheonomic and non-holonomic constraints will be treated.

3.1. Scleronomic constraints

The discretization B_m will be selected so as to satisfy the following relationship

$$\underline{\mathscr{C}}_f - \underline{\mathscr{C}}_i = B_m^T(\underline{u}_f - \underline{u}_i). \tag{6}$$

The existence of this discretization is guaranteed by the mean value theorem (Hildebrand, 1976). Indeed, considering $\underline{\mathscr{C}}(\underline{u}(t))$ to be an implicit function of time and letting $\underline{u}(t) = \underline{u}_i + (\underline{u}_f - \underline{u}_i)(t - t_i)/(t_f - t_i)$ over the time step, this theorem guarantees the existence of a time $t_\zeta \in [t_i, t_f]$ such that

$$\underline{\mathscr{C}}(\underline{u}(t_f)) = \underline{\mathscr{C}}(\underline{u}(t_i)) + \left.\frac{\partial \underline{\mathscr{C}}}{\partial \underline{u}}\right|_{t_\zeta} \frac{d\underline{u}}{dt}(t_f - t_i) = \underline{\mathscr{C}}(\underline{u}(t_i)) + \left.\frac{\partial \underline{\mathscr{C}}}{\partial \underline{u}}\right|_{t_\zeta} (\underline{u}_f - \underline{u}_i). \tag{7}$$

Clearly, the desired discretization is now

$$B_m^T = \left.\frac{\partial \underline{\mathscr{C}}}{\partial \underline{u}}\right|_{t_\zeta}. \tag{8}$$

To be complete, the scheme defined by Eqs. (4) and (5) must be augmented with the following discretized constraint equations

$$\underline{\mathscr{C}}_f = 0. \tag{9}$$

Since the same algorithm is applied at each time step, Eq. (9) also implies $\underline{\mathscr{C}}_i = 0$. Introducing these results into Eq. (6) now leads to

$$0 = \underline{\mathscr{C}}_f - \underline{\mathscr{C}}_i = B_m^T(\underline{u}_f - \underline{u}_i) = \Delta t B_m^T \frac{\underline{v}_f + \underline{v}_i}{2}, \tag{10}$$

where Eq. (5) was used. The mid-point velocity is denoted $\underline{v}_m = (\underline{v}_f + \underline{v}_i)/2$, and hence

$$\dot{\underline{\mathscr{C}}}_m = B_m^T \underline{v}_m = 0. \tag{11}$$

This result illustrates a fundamental property of the proposed algorithm: two invariants of the system are exactly satisfied, $\underline{\mathscr{C}} = 0$, Eq. (9), and $\dot{\underline{\mathscr{C}}} = 0$, Eq. (11). In other words, the proposed algorithm implies the satisfaction of the constraints at both displacement and velocity levels. The key to achieving the preservation of both invariants, is the proper selection of B_m, as defined in Eq. (6).

Next, the work done by the various forces acting on the system during a time step is evaluated by multiplying the discretized equations of motion, Eq. (4), by the displacement increment to find

$$\Delta \mathscr{W}^I + \Delta \mathscr{W}^E + \Delta \mathscr{W}^C = \Delta \mathscr{W}^A. \tag{12}$$

This equation is a statement of work balance. The work done by the inertial forces is written as

$$\Delta \mathscr{W}^I = (\underline{u}_f - \underline{u}_i)^T \underline{\mathscr{F}}_m^I = \Delta t \underline{v}_m^T \underline{\mathscr{F}}_m^I = \mathscr{K}_f - \mathscr{K}_i, \tag{13}$$

where Eq. (5) was used and the third equality defines the discretization of the inertial forces $\underline{\mathscr{F}}_m^I$. Discretizations of the inertial forces can be found in various references for rigid bodies (Simo and Wong, 1991; Simo and Tarnow, 1992), beams (Bauchau et al., 1995; Simo et al., 1995), plates and shells (Simo and Tarnow, 1994; Bauchau et al., 2002). Proceeding in a similar manner, the work done by the elastic forces is

$$\Delta \mathscr{W}^E = (\underline{u}_f - \underline{u}_i)^T \underline{\mathscr{F}}_m^E = \mathscr{V}_f - \mathscr{V}_i, \tag{14}$$

where the second equality defines the discretization of the elastic forces $\underline{\mathscr{F}}_m^E$. Discretizations of the elastic forces acting on various structural components can be found in the references cited above. The work done by the externally applied loads is simply $\Delta \mathscr{W}^A = (\underline{u}_f - \underline{u}_i)^T \underline{\mathscr{F}}_m^A$, and finally, the work done by the constraint forces is

$$\Delta \mathscr{W}^{\mathrm{C}} = (\underline{u}_{\mathrm{f}} - \underline{u}_{\mathrm{i}})^{\mathrm{T}} B_{\mathrm{m}} \underline{\lambda}_{\mathrm{m}} = (\underline{\mathscr{C}}_{\mathrm{f}} - \underline{\mathscr{C}}_{\mathrm{i}})^{\mathrm{T}} \underline{\lambda}_{\mathrm{m}} = 0, \tag{15}$$

where Eqs. (6) and (9) were used. This implies the vanishing of the work done by the discretized constraint forces, as also occurs in the exact solution. It is important to note here that the preservation of the invariants $\underline{\mathscr{C}} = 0$ and $\dot{\underline{\mathscr{C}}} = 0$, as implied by Eqs. (9) and (11), respectively, is closely related to the vanishing of the work done by the discretized constraint forces, Eq. (15). The discretization of the constraint Jacobian matrix, Eq. (6), is key to obtaining all three properties simultaneously.

Introducing Eqs. (13)–(15) into the work balance statement, Eq. (12), results in

$$(\mathscr{K}_{\mathrm{f}} + \mathscr{V}_{\mathrm{f}}) - (\mathscr{K}_{\mathrm{i}} + \mathscr{V}_{\mathrm{i}}) = \mathscr{E}_{\mathrm{f}} - \mathscr{E}_{\mathrm{i}} = \Delta \mathscr{W}^{\mathrm{A}}. \tag{16}$$

In the absence of externally applied loads, this statement implies the preservation of the total mechanical energy of the system across the time step. Since the total mechanical energy is a positive definite function of the state variables, the preservation of this quantity implies the stability of the proposed numerical scheme in the presence of constraints. In summary, the proposed algorithm consists of the discretized equation of motion, Eq. (4), the velocity-displacement relationship, Eq. (5), the definition of the constraint gradient, Eq. (6), and the constraint equation, Eq. (9).

In the proposed algorithm, the various invariants of the system are not all exactly preserved at the same instant in time. The governing equation of motion, Eq. (4), and the velocity-displacement relationship, Eq. (5), are satisfied at the mid-point $t_{\mathrm{m}} = (t_{\mathrm{f}} + t_{\mathrm{i}})/2$. The displacement level constraint, Eq. (9), is enforced at t_{f} and t_{i}, but will clearly not be satisfied at t_{m}; the same remark holds for the energy preservation statement, Eq. (16). The velocity level constraint, Eq. (11), is enforced at t_{m}. Finally, the Lagrange multipliers clearly are mid-point quantities. This contrasts with most other algorithms that enforce these various conditions at the same instant in time, typically t_{f}.

3.2. Rheonomic constraints

In the case of rheonomic constraints, the discretization B_{m} given by Eq. (6) must be modified to read

$$\underline{\mathscr{C}}_{\mathrm{f}} - \underline{\mathscr{C}}_{\mathrm{i}} = B_{\mathrm{m}}^{\mathrm{T}}(\underline{u}_{\mathrm{i}}, \underline{u}_{\mathrm{f}}, t)(\underline{u}_{\mathrm{f}} - \underline{u}_{\mathrm{i}}) + \underline{a}_{\mathrm{m}}(\underline{u}_{\mathrm{i}}, \underline{u}_{\mathrm{f}}, t). \tag{17}$$

Here again, the existence of this discretization is guaranteed by the mean value theorem. The scheme defined by Eqs. (4) and (5) is augmented with the discretized constraint equations (9). This leads to

$$0 = \underline{\mathscr{C}}_{\mathrm{f}} - \underline{\mathscr{C}}_{\mathrm{i}} = B_{\mathrm{m}}^{\mathrm{T}}(\underline{u}_{\mathrm{f}} - \underline{u}_{\mathrm{i}}) + \underline{a}_{\mathrm{m}} = \Delta t B_{\mathrm{m}}^{\mathrm{T}} \underline{v}_{\mathrm{m}} + \underline{a}_{\mathrm{m}} = \dot{\underline{\mathscr{C}}}_{\mathrm{m}} = 0. \tag{18}$$

Here again, the proposed algorithm implies the satisfaction of the constraints at both displacement and velocity levels. Finally, the work done the forces of constraint is

$$\Delta \mathscr{W}^{\mathrm{C}} = (\underline{u}_{\mathrm{f}} - \underline{u}_{\mathrm{i}})^{\mathrm{T}} B_{\mathrm{m}} \underline{\lambda}_{\mathrm{m}} = \left[(\underline{u}_{\mathrm{f}} - \underline{u}_{\mathrm{i}})^{\mathrm{T}} B_{\mathrm{m}} + \underline{a}_{\mathrm{m}}^{\mathrm{T}} \right] \underline{\lambda}_{\mathrm{m}} - \underline{a}_{\mathrm{m}}^{\mathrm{T}} \underline{\lambda}_{\mathrm{m}}. \tag{19}$$

Introducing Eq. (18) then leads to

$$\Delta \mathscr{W}^{\mathrm{C}} = (\underline{\mathscr{C}}_{\mathrm{f}} - \underline{\mathscr{C}}_{\mathrm{i}})^{\mathrm{T}} \underline{\lambda}_{\mathrm{m}} - \underline{a}_{\mathrm{m}}^{\mathrm{T}} \underline{\lambda}_{\mathrm{m}} = -\underline{a}_{\mathrm{m}}^{\mathrm{T}} \underline{\lambda}_{\mathrm{m}}. \tag{20}$$

Clearly, the forces associated with rheonomic constraints do work. The work balance statement, Eq. (16) now becomes

$$\mathscr{E}_{\mathrm{f}} = \mathscr{E}_{\mathrm{i}} + \Delta \mathscr{W}^{\mathrm{A}} - \Delta \mathscr{W}^{\mathrm{C}}, \tag{21}$$

which is the correct work balance statement for systems involving rheonomic constraints.

3.3. Non-holonomic constraints

The treatment of non-holonomic constraints within the framework of the proposed algorithm is rather straightforward. The scheme defined by Eqs. (4) and (5) is augmented with the following discretized constraint equations

$$\underline{\mathscr{C}}_{\mathrm{m}} = B_{\mathrm{m}}^{\mathrm{T}}(\underline{u}_{\mathrm{i}}, \underline{u}_{\mathrm{f}}, t)\underline{v}_{\mathrm{m}} + \underline{a}_{\mathrm{m}}(\underline{u}_{\mathrm{i}}, \underline{u}_{\mathrm{f}}, t) = 0. \tag{22}$$

In this case, B_{m} is simply a second order accurate approximation of the constraint Jacobian matrix. The evaluation of the work done by the non-holonomic constraints closely follows that of the work done by rheonomic constraints. In fact, it is readily shown that Eqs. (20) and (21) also hold for non-holonomic constraints.

4. The energy decaying algorithm

The proposed algorithm is extended to a numerically dissipative scheme with the following discretization of the equations of motion

$$\underline{\mathscr{F}}_g^{\mathrm{I}} + \underline{\mathscr{F}}_g^{\mathrm{E}} + B_g\underline{\lambda}_g = \underline{\mathscr{F}}_g^{\mathrm{A}}; \tag{23}$$

$$\underline{\mathscr{F}}_h^{\mathrm{I}} + \underline{\mathscr{F}}_h^{\mathrm{E}} - \tfrac{1}{3}[B_g - B_h]\underline{\lambda}_g = \underline{\mathscr{F}}_h^{\mathrm{A}}. \tag{24}$$

The velocity-displacement relationship are approximated as

$$\frac{\underline{u}_{\mathrm{f}} - \underline{u}_{\mathrm{i}}}{\Delta t} = \frac{\underline{v}_{\mathrm{f}} + \underline{v}_j}{2}, \tag{25}$$

$$3\frac{\underline{u}_j - \underline{u}_{\mathrm{i}}}{\Delta t} = -\frac{1}{2}\left[(\underline{v}_{\mathrm{f}} - \underline{v}_{\mathrm{i}}) - \alpha(\underline{v}_j - \underline{v}_{\mathrm{i}})\right], \tag{26}$$

where α is a coefficient that control the amount of numerical dissipation in the algorithm. In these equations, subscripts $(\cdot)_j$ indicate the value of a specific quantity at an intermediate time t_j; subscripts $(\cdot)_g$ and $(\cdot)_h$ indicate the "mid-point value" of the corresponding quantity within time intervals $[t_j, t_{\mathrm{f}}]$ and $[t_{\mathrm{i}}, t_j]$, respectively. The discretized inertial and elastic forces can be derived from their counterparts in the EP algorithm following the procedure described in (Bauchau, 1998; Bauchau et al., 2003). For simplicity of the exposition, the case of holonomic constraints will be treated here; extending this work to other constraint types is straightforward. The discretization B_g and B_h will be selected so as to satisfy the following relationships

$$\underline{\mathscr{C}}_{\mathrm{f}} - \underline{\mathscr{C}}_j = B_g^{\mathrm{T}}(\underline{u}_{\mathrm{f}} - \underline{u}_j), \tag{27}$$

$$\underline{\mathscr{C}}_j - \underline{\mathscr{C}}_{\mathrm{i}} = B_h^{\mathrm{T}}(\underline{u}_j - \underline{u}_{\mathrm{i}}). \tag{28}$$

Note that these relationships are identical to Eq. (6) but expressed with different sets of subscripts. To be complete, the scheme defined by Eqs. (23)–(28) must be augmented with the discretized constraint equations, Eq. (9). Introducing these results into Eq. (6) now leads to

$$0 = \underline{\mathscr{C}}_{\mathrm{f}} - \underline{\mathscr{C}}_j + \underline{\mathscr{C}}_j - \underline{\mathscr{C}}_{\mathrm{i}} = B_g^{\mathrm{T}}(\underline{u}_{\mathrm{f}} - \underline{u}_j) + B_h^{\mathrm{T}}(\underline{u}_j - \underline{u}_{\mathrm{i}}) = \Delta t B_g^{\mathrm{T}}\underline{v}_g - (B_g^{\mathrm{T}} - B_h^{\mathrm{T}})(\underline{u}_j - \underline{u}_{\mathrm{i}}), \tag{29}$$

where Eqs. (25) and (26) were used. This relationship represents the vanishing of the algorithmic mid-point velocity.

Next, the work done by the various forces acting on the system during a time step is evaluated from Eqs. (23) and (24) to find the work balance statement, Eq. (12). Discretization of the inertial and elastic forces can be found in various references for beams (Bauchau et al., 1995; Bauchau and Theron, 1996; Bottasso et al., 2001a,b), plates and shells (Bauchau and Bottasso, 1999; Bauchau et al., 2002). The work they perform is found to be

$$\Delta\mathscr{W}^{\mathrm{I}} = \mathscr{K}_{\mathrm{f}} - \mathscr{K}_{\mathrm{i}} + \frac{\alpha}{2}c^{\mathrm{I2}} \tag{30}$$

and

$$\Delta\mathscr{W}^{\mathrm{E}} = \mathscr{V}_{\mathrm{f}} - \mathscr{V}_{\mathrm{i}} + \frac{\alpha}{2}c^{\mathrm{E2}}, \tag{31}$$

respectively, where c^{I2} and c^{E2} are positive constants. The work done by the externally applied loads is simply $\Delta\mathscr{W}^{\mathrm{A}} = (\underline{u}_{\mathrm{f}} - \underline{u}_{\mathrm{i}}^{\mathrm{T}})\underline{\mathscr{F}}_g^{\mathrm{A}} + 3(\underline{u}_j - \underline{u}_{\mathrm{i}})\underline{\mathscr{F}}_h^{\mathrm{A}}$, and, in view of Eqs. (27), (28) and (9), the work done by the constraint forces vanishes

$$\Delta\mathscr{W}^{\mathrm{C}} = \left[(\underline{u}_{\mathrm{f}} - \underline{u}_{\mathrm{i}})^{\mathrm{T}}B_g - (\underline{u}_j - \underline{u}_{\mathrm{i}})^{\mathrm{T}}(B_g - B_h)\right]\underline{\lambda}_g = \left[(\underline{\mathscr{C}}_{\mathrm{f}} - \underline{\mathscr{C}}_j)^{\mathrm{T}} + (\underline{\mathscr{C}}_j - \underline{\mathscr{C}}_{\mathrm{i}})^{\mathrm{T}}\right]\underline{\lambda}_g = 0. \tag{32}$$

Introducing Eqs. (30)–(32) into the work balance statement, Eq. (12), results in

$$\mathscr{E}_{\mathrm{f}} - \mathscr{E}_{\mathrm{i}} = \Delta\mathscr{W}^{\mathrm{A}} - \frac{\alpha}{2}c^2, \tag{33}$$

where $c^2 = c^{\mathrm{I2}} + c^{\mathrm{E2}}$. In the absence of externally applied loads, this statement implies the decay of the total mechanical energy of the system across the time step and the stability of the proposed numerical scheme in the presence of constraints. In summary, the proposed algorithm consists of the discretized equations of motion, Eqs. (23) and (24), the velocity-displacement relationship, Eqs. (25) and (26), the definition of the constraint gradients, Eqs. (27) and (28), and the constraint equation, Eq. (9).

5. Relationship with the GGL stabilization method

Gear et al. (1985) proposed a constraint stabilization technique, called stabilized index-2 or GGL method, based on the reduction of the governing equations from index-3 to index-2 DAEs. For simplicity of the exposition, the case of scleronomic, holonomic constraints will be presented. The equations of motion are written in the following form for the force equilibrium equations

$$\underline{\mathscr{F}}^{\mathrm{I}}(\underline{u}, \underline{v}, \dot{\underline{v}}) + \underline{\mathscr{F}}^{\mathrm{E}}(\underline{u}) + B(\underline{u})\underline{\lambda} = \underline{\mathscr{F}}^{\mathrm{A}}, \tag{34}$$

the velocity-displacement relationships,

$$\dot{\underline{u}} - \underline{v} + B(\underline{u})\underline{\mu} = 0, \tag{35}$$

and the constraint equations enforced at both displacement and velocity levels

$$\underline{\mathscr{C}}(\underline{u}) = 0; \quad B(\underline{u})\underline{v} = 0. \tag{36}$$

Gear et al. (1985) have shown that the system of Eqs. (34)–(36) forms a set of index-2 DAEs and its solution is identical to that of the system of index-3 DAEs formed by Eqs. (1) and (3). Furthermore, $\underline{\mu} = 0$ is an invariant for the exact solution. This result is easily understood: the Lagrange multipliers $\underline{\mu}$ are used to enforce the velocity level constraints, $B\underline{v} = 0$. However, in the exact solution, velocity level constraints are implied by displacement level constraints, and hence, the corresponding Lagrange multipliers vanish since they enforce redundant constraints. In the numerical world however, the satisfaction of displacement level constraints does not automatically imply that of velocity level constraints, and $\underline{\mu} \neq 0$.

Consider the following discretization of the index-2 set of DAEs, Eqs. (34)–(36): discretized equilibrium equation (4), constraint Eqs. (9) and (11), and velocity-displacement relationship

$$\frac{\underline{u}_{\mathrm{f}} - \underline{u}_{\mathrm{f}}}{\Delta t} - \underline{v}_{\mathrm{m}} + B_{\mathrm{m}}\underline{\mu}_{\mathrm{m}} = 0, \tag{37}$$

where B_{m} is defined by Eq. (6). Multiplying this last equation by $B_{\mathrm{m}}^{\mathrm{T}}$ results in

$$B_{\mathrm{m}}^{\mathrm{T}}\frac{\underline{u}_{\mathrm{f}} - \underline{u}_{\mathrm{f}}}{\Delta t} - B_{\mathrm{m}}^{\mathrm{T}}\underline{v}_{\mathrm{m}} + B_{\mathrm{m}}^{\mathrm{T}}B_{\mathrm{m}}\underline{\mu}_{\mathrm{m}} = 0. \tag{38}$$

The first term vanishes in view of Eqs. (6) and (9), whereas Eq. (11) implies the vanishing of the second term. Consequently, $B_{\mathrm{m}}^{\mathrm{T}}B_{\mathrm{m}}\underline{\mu}_{\mathrm{m}} = 0$, where $B_{\mathrm{m}}^{\mathrm{T}}B_{\mathrm{m}}$ is positive definite since B_{m} has full rank. It follows that $\underline{\mu}_{\mathrm{m}} = 0$, i.e. the numerical solution shares this invariant with the exact solution.

In summary, the index-2 set of DAEs proposed by Gear, Eqs. (34)–(36), discretized by Eqs. (4), (37), (9) and (11), respectively, implies $\underline{\mu}_{\mathrm{m}} = 0$. However, if $\underline{\mu}_{\mathrm{m}} = 0$, these latter equations are identical to the proposed algorithm defined by Eqs. (4), (5), (9) and (11). Hence, the proposed scheme can be interpreted as the discretization of a set of index-2 DAEs that evolves over the invariant manifold $\underline{\mu} = 0$. In other words, the algorithm is "self-stabilized".

In view of Eq. (37), it should be noted that the use of the mid point rule for the velocity-displacement relationship, Eq. (5), is sufficient to guarantee $\mu_{\mathrm{m}} = 0$. However, this choice is clearly not sufficient to achieve stabilization of the constraints. In the original work of Gear et al. (1985) the GGL scheme was developed to enable the satisfaction of the velocity constraint at the final time, in the same way that the position constraint is to be satisfied. Numerical dissipation was used to stabilize the resulting system, and the additional Lagrange multiplier μ does not vanish. In the present approach, the velocity constraint is not imposed at the final time, together with the position constraint, but rather at the midpoint. This key difference enables achieving constraint stabilization without resorting to numerical dissipation and without introducing an additional Lagrange multiplier. This seems to suggest that imposing both position and velocity constraints at the same instant in time over-constrains the system.

6. Numerical examples

6.1. The rigid body

Consider the rigid body depicted in Fig. 1. The position vector of its reference point **O** is denoted $\underline{u}$ and its orientation is determined by an orthonormal basis $\mathscr{B} := (\overline{e}_1, \overline{e}_2, \overline{e}_3)$. The position vector of an arbitrary point **P** of the rigid body is then $\underline{x}_P = \underline{u} + s_1^*\overline{e}_1 + s_2^*\overline{e}_2 + s_3^*\overline{e}_3$, where $\underline{s}^*$ are the components of the position vector of point **P** with respect to point **O**, measured in $\mathscr{B}$. The kinetic energy of the rigid body is readily found as $\mathscr{K} = \frac{1}{2}\dot{\underline{d}}^{\mathrm{T}}M^*\dot{\underline{d}}$, where array $\underline{d}$ stores the degrees of freedom of the system $\underline{d}^{\mathrm{T}} = [\underline{u}^{\mathrm{T}}, \overline{e}_1^{\mathrm{T}}, \overline{e}_2^{\mathrm{T}}, \overline{e}_3^{\mathrm{T}}]$, and the mass matrix is

$$M^* = \begin{bmatrix} M_{00}I & M_{01}I & M_{02}I & M_{03}I \\ M_{01}I & M_{11}I & M_{12}I & M_{13}I \\ M_{02}I & M_{12}I & M_{22}I & M_{23}I \\ M_{03}I & M_{13}I & M_{23}I & M_{33}I \end{bmatrix}. \tag{39}$$

I denote the 3×3 identity matrix, $M_{00} = \int_V \rho\,\mathrm{d}V$ is the total of the body, where ρ is the material density and V the volume of the body. $M_{0\mathrm{i}} = \int_V \rho s_{\mathrm{i}}^*\,\mathrm{d}V$ then defines the first moments of inertia of the body, and $M_{ij} = \int_V \rho s_{\mathrm{i}}^* s_j^*\,\mathrm{d}V$ is closely related to the tensor of moments of inertia.

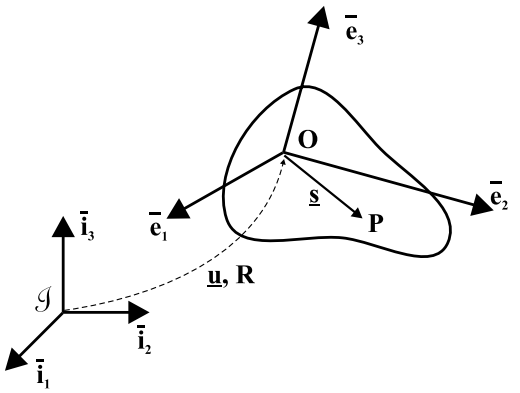

Fig. 1. Configuration of the rigid body.

The kinematics of the rigid body is defined by the twelve degrees of freedom stored in array $\underline{d}$. Clearly, six constraints must be imposed: three conditions on the normality of vectors $\bar{e}_1$, $\bar{e}_2$ and $\bar{e}_3$, and three additional constraints enforcing their orthogonality. The array of constraints writes

$$\underline{\mathscr{C}} = \begin{bmatrix} (\bar{e}_1^{\mathrm{T}}\bar{e}_1 - 1)/2 \\ (\bar{e}_2^{\mathrm{T}}\bar{e}_2 - 1)/2 \\ (\bar{e}_3^{\mathrm{T}}\bar{e}_3 - 1)/2 \\ \bar{e}_2^{\mathrm{T}}\bar{e}_3 \\ \bar{e}_1^{\mathrm{T}}\bar{e}_3 \\ \bar{e}_1^{\mathrm{T}}\bar{e}_2 \end{bmatrix}. \tag{40}$$

The equations of motion of the system are then $M^*\ddot{\underline{d}} + B\underline{\lambda} = \underline{F}$, where $\underline{\lambda}$ is an array of six Lagrange multipliers, $\underline{F}$ the array of externally applied forces and B the constraint Jacobian matrix

$$B(\bar{e}_1, \bar{e}_2, \bar{e}_3) = \begin{bmatrix} 0 & 0 & 0 & 0 & 0 & 0 \\ \bar{e}_1 & 0 & 0 & 0 & \bar{e}_3 & \bar{e}_2 \\ 0 & \bar{e}_2 & 0 & \bar{e}_3 & 0 & \bar{e}_1 \\ 0 & 0 & \bar{e}_3 & \bar{e}_2 & \bar{e}_1 & 0 \end{bmatrix}. \tag{41}$$

The discretized equations of motion then become $M^*(\underline{v}_{\mathrm{f}} - \underline{v}_{\mathrm{i}})/\Delta t + B(\bar{e}_{1\mathrm{m}}, \bar{e}_{2\mathrm{m}}, \bar{e}_{3\mathrm{m}})\underline{\lambda}_{\mathrm{m}} = \underline{F}_{\mathrm{m}}$, where $\bar{e}_{km} = (\bar{e}_{ki} + \bar{e}_{kf})/2$; the velocity-displacement relationship $(\underline{d}_{\mathrm{f}} - \underline{d}_{\mathrm{i}})/\Delta t = (\underline{v}_{\mathrm{f}} + \underline{v}_{\mathrm{i}})/2$, and the constraint equation, Eq. (9). It is readily verified that $B^{\mathrm{T}}(\bar{e}_{1\mathrm{m}}, \bar{e}_{2\mathrm{m}}, \bar{e}_{3\mathrm{m}})(\underline{d}_{\mathrm{f}} - \underline{d}_{\mathrm{i}}) = \underline{\mathscr{C}}_{\mathrm{f}} - \underline{\mathscr{C}}_{\mathrm{i}}$, as required by condition (6).

A rigid body with the following properties was simulated: $M_{00} = 1.8$ kg, $(M_{01}, M_{02}, M_{03}) = (0.18, -0.72, 0.54)$ kg m, $(M_{11}, M_{22}, M_{33}) = (0.2, 0.7, 0.4)$ kg m^2, and $(M_{12}, M_{13}, M_{23}) = (-0.012, 0.015, -0.023)$ kg m^2. The rigid body had an initial velocity $\underline{v}_0^{\mathrm{T}} = [5, 0, 0]$ m/s and initial angular velocity $\underline{\omega}_0^{\mathrm{T}} = [0, 4, 0]$ rad/s. The configuration of the rigid body was computed for 5 s period using the proposed EP algorithm with a constant time step $\Delta t = 0.0125$ s. Fig. 2 shows the components of vectors $\bar{e}_1$ and $\bar{e}_2$, whereas Fig. 3 depicts the angular velocity vector and the first three Lagrange multipliers, λ_{11}, λ_{22}, and λ_{33}. The displacement and velocity level constraints for each of the six constraints were satisfied to machine accuracy, as was the energy preservation condition. These results illustrate the performance obtained using the EP algorithm: stable predictions are obtained without resorting to a dissipative algorithm; none of the computed quantities exhibit oscillations of a numerical origin. Next, the ED scheme was used for this problem and its predictions were in excellent agreement with those of the EP algorithm. Fig. 4 shows the results of a convergence study performed for both EP and ED schemes. The displacement, velocity, and

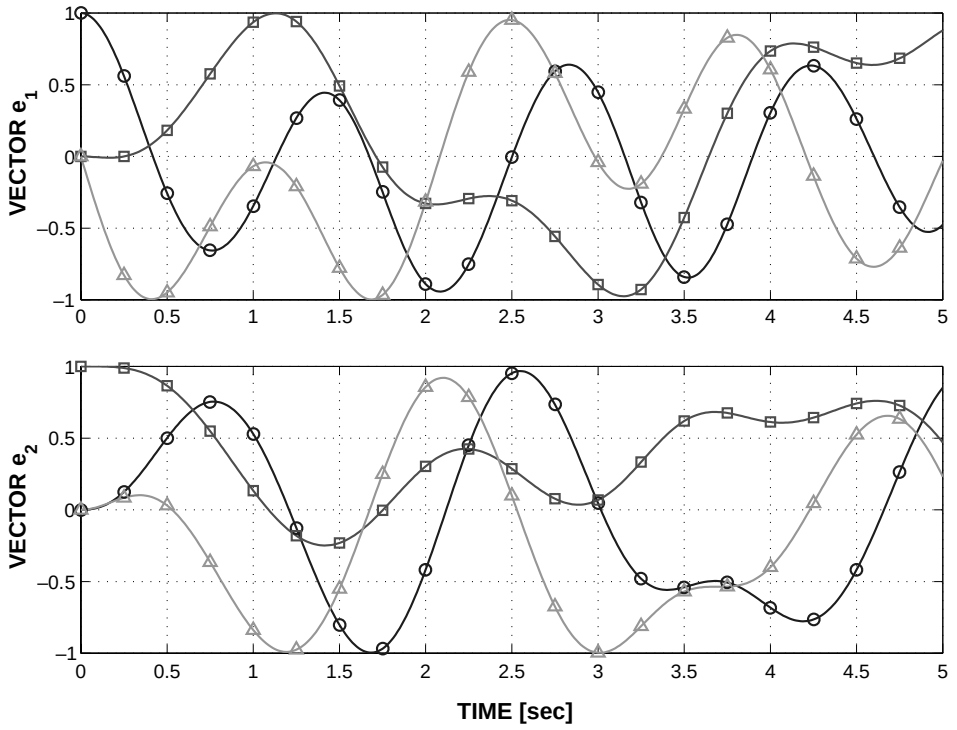

Fig. 2. Time history of the orientation vector $\bar{e}_1$ (top figure) and $\bar{e}_2$ (bottom figure). Components along $\bar{\imath}_1$ (○), $\bar{\imath}_2$ (□) and $\bar{\imath}_3$ (△).

mid-point Lagrange multiplier components all exhibit quadratic or cubic convergence rates for the EP and ED algorithms, respectively.

6.2. The rigid body/universal joint system

The second example deal with a rigid body attached to the ground by means of a universal joint, as depicted in Fig. 5. The upper component of a universal joint is connected to an inertial point **O** and rotates at a constant angular velocity Ω with respect to an inertial basis $\mathscr{I} := (\bar{\imath}_1, \bar{\imath}_2, \bar{\imath}_3)$ such that $\bar{d}_1(t) = \cos(\Omega t)\bar{\imath}_1 - \sin(\Omega t)\bar{\imath}_3$. The lower component of the universal joint connects at point $\mathbf{O}'$ to a rigid body with an attached orthonormal basis $\mathscr{B} := (\bar{e}_1, \bar{e}_2, \bar{e}_3)$. Points **O** and $\mathbf{O}'$ are coincident. The kinematics of the universal joint impose the orthogonality of unit vectors $\bar{d}_1$ and $\bar{e}_3$, i.e. the rheonomic holonomic constraint $\mathscr{C} = \bar{e}_3^{\mathrm{T}}\bar{d}_1(t) = 0$. The position vector of the center of mass of the rigid body with respect to point $\mathbf{O}'$ is denoted $\underline{\eta}$. Gravity acts on the system as indicated in Fig. 5.

The equations of motion of the system are readily found as $(R\underline{h}^*)^{\cdot} + \lambda\tilde{e}_3\underline{d}_1 + m_0\tilde{g}\underline{\eta} = 0$, where R is the rotation tensor from $\mathscr{I}$ to $\mathscr{B}$ measured in $\mathscr{I}$, $\underline{h}^* = I^*\underline{\omega}^*$ are the components of the angular momentum vector in the material system $\mathscr{B}$, λ is the Lagrange multiplier, m_0 the total mass of the body, and $\underline{g}$ the acceleration of gravity vector. The tensor of moments of inertia of the rigid body with respect to point $\mathbf{O}'$ measured in $\mathscr{B}$ is denoted I^*, and the angular velocity vector in the material system is $\underline{\omega}^*$.

Although the existence of a discretization of the constraint gradient array that satisfies Eq. (6) is guaranteed by the mean value theorem, it is not always easy to find an analytical expression for B_{m}. In practice, it can be constructed in the following manner

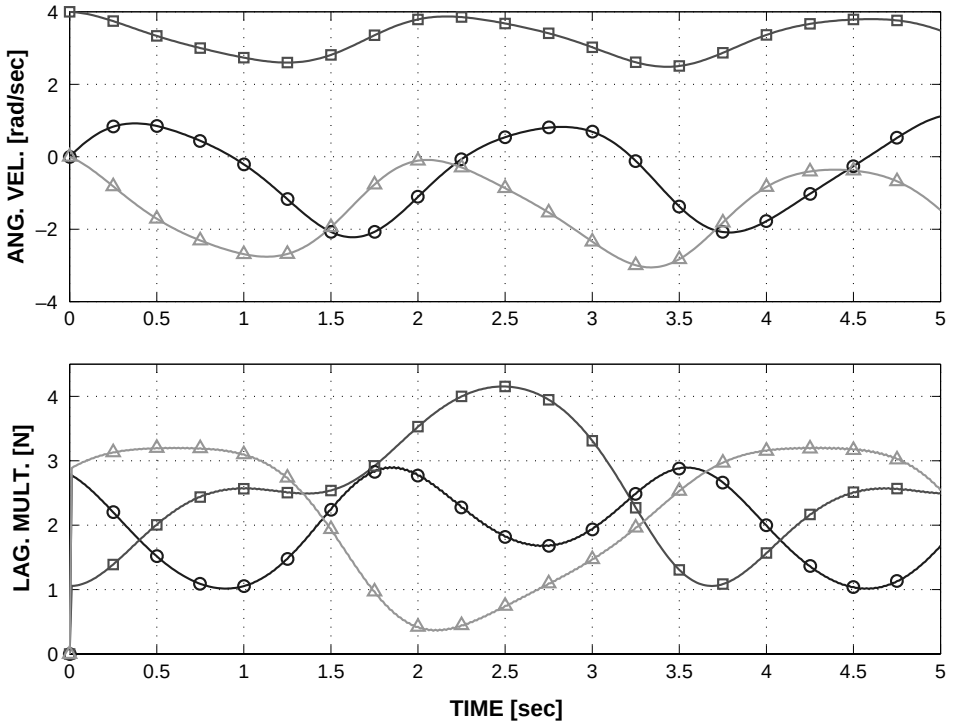

Fig. 3. Top figure: time history of the angular velocity vector; component along $\bar{\imath}_1$ (○), $\bar{\imath}_2$ (□) and $\bar{\imath}_3$ (△). Bottom figure: time history of the Lagrange multipliers; component λ_{11} (○), λ_{22} (□), λ_{33} (△).

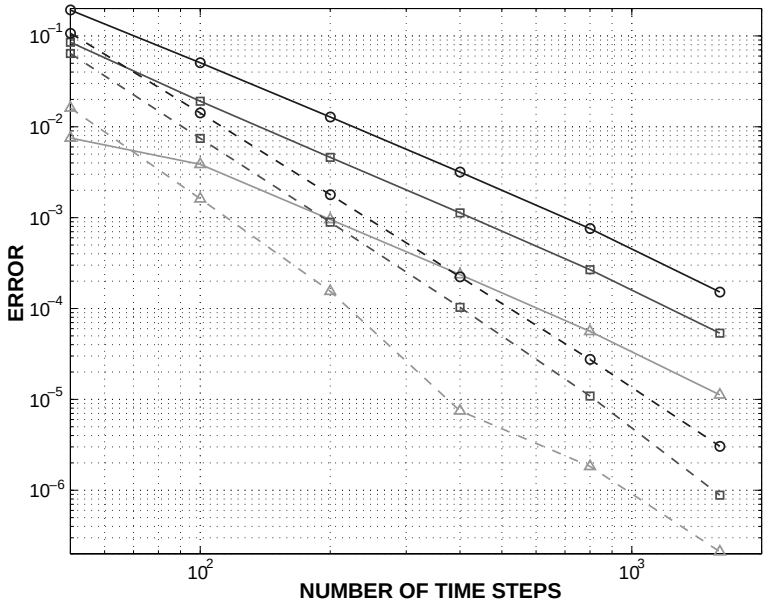

Fig. 4. Convergence of the orientation vector $\bar{e}_1$ (○), angular velocity vector (□), and mid-point Lagrange multiplier λ_{11} (△) for the rigid body problem. EP algorithm: solid line; ED algorithm: dashed line.

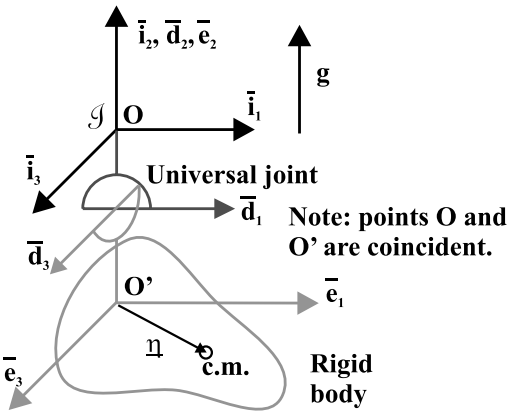

Fig. 5. Configuration of the rigid body connected to a universal joint.

$$\mathscr{C}_{\mathrm{f}} - \mathscr{C}_{\mathrm{i}} = \overline{d}_{1\mathrm{f}}^{\mathrm{T}}\overline{e}_{3\mathrm{f}} - \overline{d}_{1\mathrm{i}}^{\mathrm{T}}\overline{e}_{3\mathrm{i}} = \overline{d}_{1\mathrm{f}}^{\mathrm{T}}\left(1 + \frac{\tilde{r}}{2}\right)\overline{e}_{3\mathrm{m}} - \overline{d}_{1\mathrm{i}}^{\mathrm{T}}\left(1 - \frac{\tilde{r}}{2}\right)\overline{e}_{3\mathrm{m}}, \tag{42}$$

where $\underline{r}$ are the Rodrigues parameter (see Appendix A) of the incremental rotation tensor from R_{i} to R_{f}, and $\overline{e}_{3\mathrm{m}} = (\overline{e}_{3\mathrm{f}} + \overline{e}_{3\mathrm{i}})/2$. It then follows that

$$\mathscr{C}_{\mathrm{f}} - \mathscr{C}_{\mathrm{i}} = \underline{r}^{\mathrm{T}}\tilde{e}_{3\mathrm{m}}\underline{d}_{1\mathrm{m}} + \overline{e}_{3\mathrm{m}}^{\mathrm{T}}(\overline{d}_{1\mathrm{f}} - \overline{d}_{1\mathrm{i}}), \tag{43}$$

where $\overline{d}_{1\mathrm{m}} = (\overline{d}_{1\mathrm{i}} + \overline{d}_{1\mathrm{f}})/2$. Comparing this relationship with Eq. (6), it is clear that $\underline{B}_{\mathrm{m}} = \tilde{e}_{3\mathrm{m}}\overline{d}_{1\mathrm{m}}$; the second term corresponds to the discretization of $\mathrm{d}\mathscr{C}/\mathrm{d}t$, since this is a time dependent constraint. Following a similar path, the change in the potential of the gravity load, $\mathscr{V} = m_0\underline{g}^{\mathrm{T}}\underline{\eta}$, can be expressed as

$$\mathscr{V}_{\mathrm{f}} - \mathscr{V}_{\mathrm{i}} = m_0\underline{g}^{\mathrm{T}}(\underline{\eta}_{\mathrm{f}} - \underline{\eta}_{\mathrm{i}}) = m_0\underline{g}^{\mathrm{T}}\tilde{r}\underline{\eta}_{\mathrm{m}} = -\underline{r}^{\mathrm{T}}m_0\tilde{g}\underline{\eta}_{\mathrm{m}}, \tag{44}$$

where Eqs. (A.2) and (A.3) were used. These developments suggest the following discretization of the equations of motion

$$\frac{R_{\mathrm{f}}\underline{h}_{\mathrm{f}}^{*} - R_{\mathrm{i}}\underline{h}_{\mathrm{i}}^{*}}{\Delta t} + \lambda_{\mathrm{m}}\tilde{e}_{3\mathrm{m}}\underline{d}_{1\mathrm{m}} + m_0\tilde{g}\underline{\eta}_{\mathrm{m}} = 0, \tag{45}$$

supplemented by velocity-displacement relationship: $\underline{\omega}_{\mathrm{m}}^{*} = R_{\mathrm{i}}^{\mathrm{T}}\underline{r}/\Delta t$. As discussed in Section 3.2, rheonomic constraints can perform work, see Eq. (20). The work done by the driving torque at the universal joint is $\Delta\mathscr{W}^{\mathrm{C}} = -\lambda_{\mathrm{m}}\overline{e}_{3\mathrm{m}}^{\mathrm{T}}(\overline{d}_{1\mathrm{f}} - \overline{d}_{1\mathrm{i}})$.

A rigid body with the following properties was simulated: total mass, $m_0 = 1.8$ kg, center of mass location, $\underline{\eta} = (0.1, -0.4, 0.3)$ m, moments of inertia, $(I_{11}^{*}, I_{22}^{*}, I_{33}^{*}) = (1.1, 0.6, 0.9)$ kg m^2, and $(I_{12}^{*}, I_{13}^{*}, I_{23}^{*}) = (0.012, -0.015, 0.023)$ kg m^2. The prescribed angular velocity is $\Omega = 1.0$ rad/s and $g = 9.81$ m/s^2. The system was modeled for a complete revolution of the universal joint using the EP scheme; 400 equal time step were used.

Fig. 6 shows the orientation and angular velocity of the rigid body as a function of the non-dimensional time $\tau = \Omega t/2\pi$. The orientation of the body is represented by the components of the conformal rotation vector, and the sudden changes in their values correspond to rescaling operations that circumvent the singularities associated with the conformal rotation vector (Bauchau and Trainelli, in press). Note that the angular velocity of the body rapidly increases from its initial unit value under the combined effects of the driving torque and gravity loading. Fig. 7 depicts the magnitudes of the Lagrange multiplier and driving

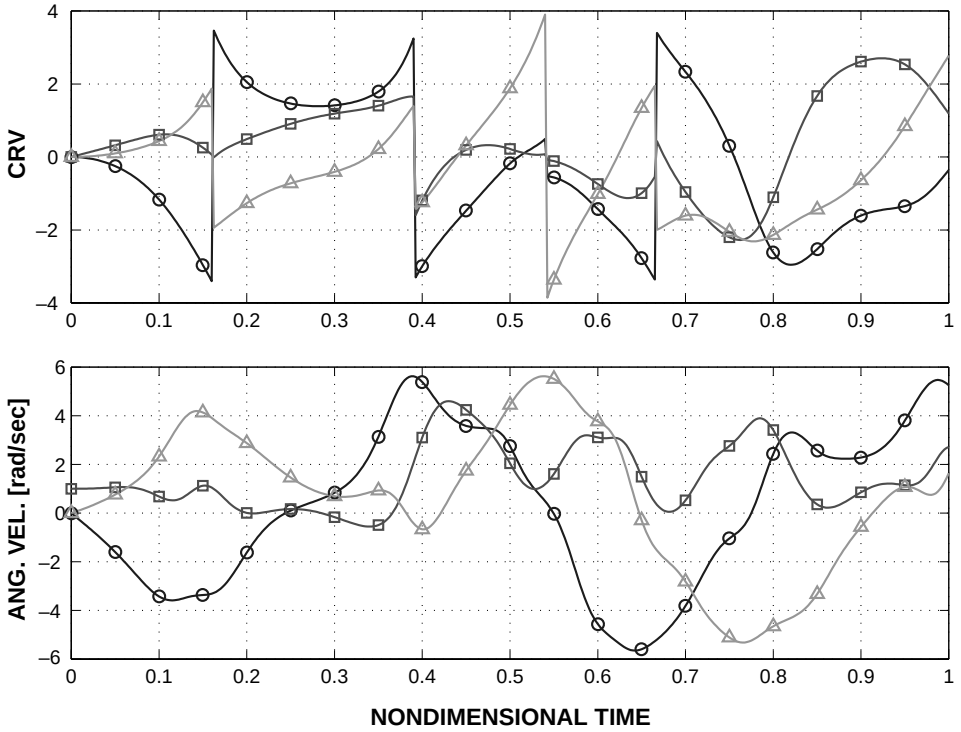

Fig. 6. Time history of the rigid body conformal rotation vector (top figure) and angular velocity vector (bottom figure). Components along $\bar{\imath}_1$ (○), $\bar{\imath}_2$ (□) and $\bar{\imath}_3$ (△).

torque. Here again, the computation is stable and all predicted quantities present smooth time histories although the algorithm features no numerical dissipation.

6.3. The wind turbine system

The last example deals the two-bladed wind turbine mounted on an elastic tower, as depicted in Fig. 8 that also details the connections between the various components of the system. The physical properties are described by Stol et al. (1999). The elastic tower, modeled with four cubic beam element, is connected at point **T** to the bed plate, modeled with a single cubic beam element, by means of a revolute joint (labeled Rvj yaw in the figure). A revolute joint (Rvj tilt) then connects the bed plate to the nacelle, modeled with a single cubic beam element, at point **S**. In turn, the shaft, modeled with a single cubic beam element, is connected to the nacelle through a revolute joint (Rvj shaft). Finally, a last revolute joint (Rvj teeter) attaches the hub and blades assembly to the shaft at point **E**. The hub is modeled as a rigid body, while each of the two blades are modeled with six cubic beam elements, respectively. The model involved 360 degrees of freedom associated with the 60 nodes defining the beam elements (6 degrees of freedom per node, three displacements and three rotations). Details about the formulation of the beam element can be found in (Bauchau, 1998; Bauchau et al., 2003). In addition, 12 Lagrange multipliers were associated with the revolute joints (three Lagrange multipliers for each of the four revolute joints). Finally, three constraints were used to connect the hub to each of the two blades. The complete system involved 378 degrees of freedom, of which 18 were Lagrange multipliers.

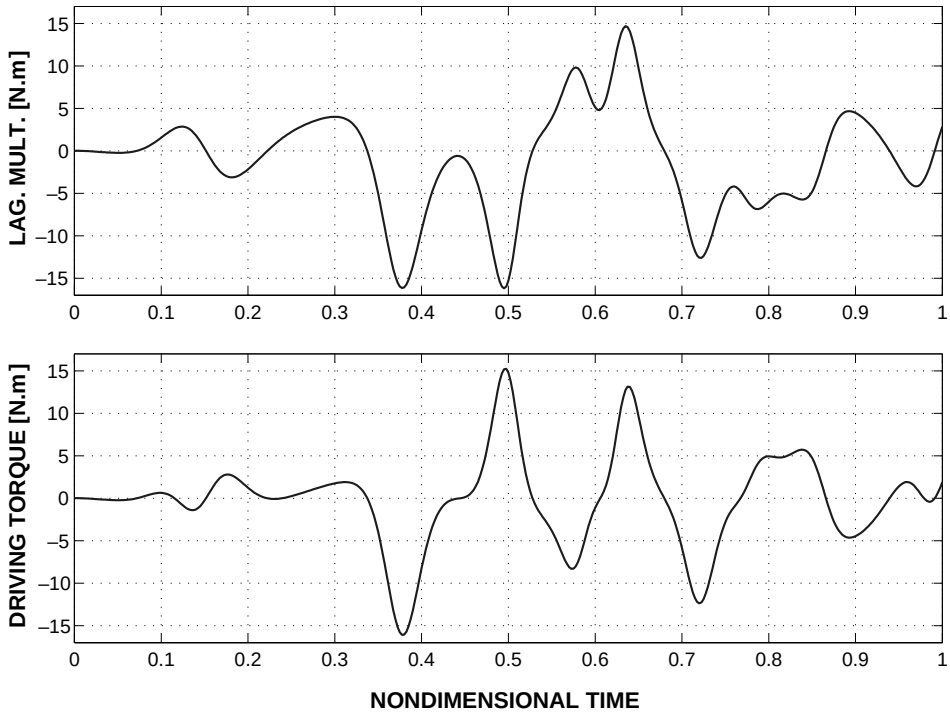

Fig. 7. Time history of the Lagrange multiplier (top figure) and driving torque (bottom figure).

The angular velocity of the rotor was prescribed to $\Omega = 6$ rad/s, and two concentrated loads were applied at the tip of the blades. The time history of these loads was

$$P(t) = \begin{cases} P_0(1 - \cos\pi t)/2 & t \leqslant 2, \\ 0 & t > 2, \end{cases} \tag{46}$$

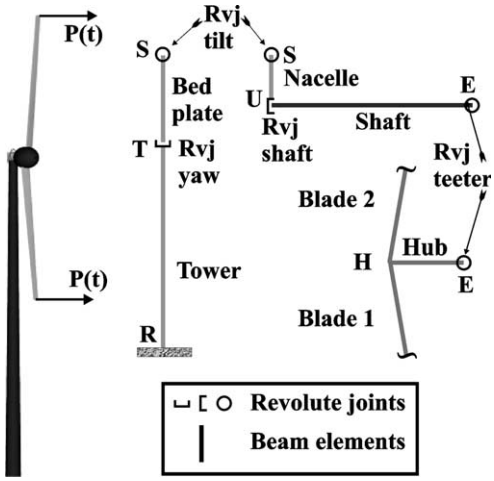

Fig. 8. The wind turbine problem.

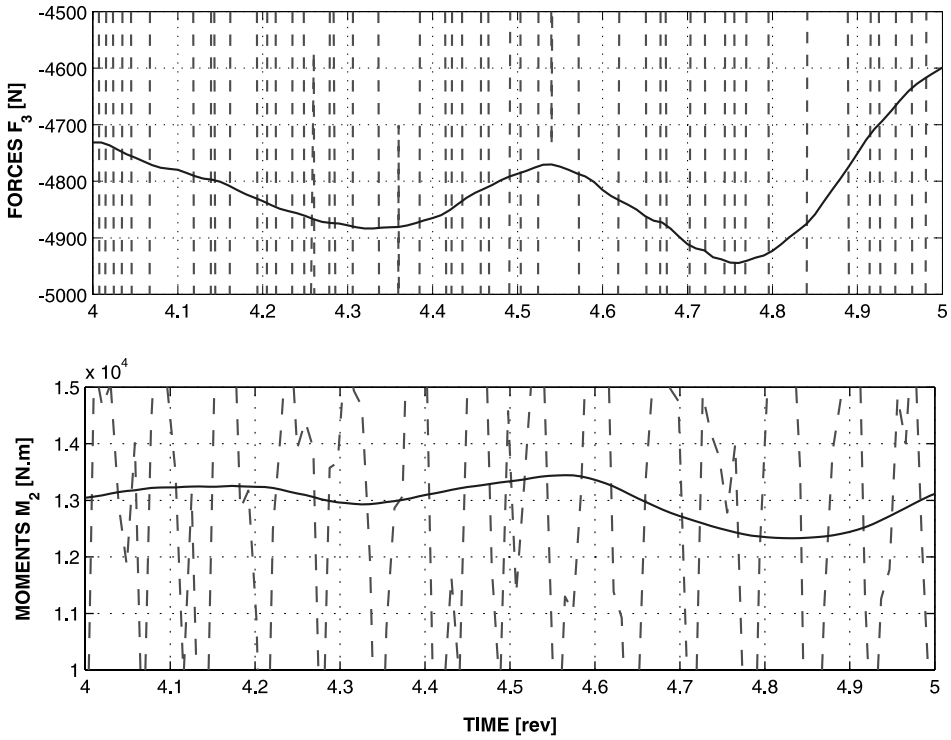

Fig. 9. Time history of the mid-span shear force F_3 (top figure) and bending moment M_3 (bottom figure) in the blade. ED scheme: solid line; EP scheme: dashed line.

where $P_0 = 1$ kN. The dynamic response of the system was computed for 10 revolutions of the rotor using a constant time step $\Delta t = 5 \times 10^{-03}$ s. Due to the high centrifugal stiffening of the blades associated with the spinning of the rotor, the system is stiff. At first, the EP scheme was used to integrate the equations of motion. The predicted blade mid-span shear force and bending moment are shown in Fig. 9. This integrator is unable to cope with the high stiffness of the system and violent oscillations are observed at each time step. The predictions of the ED schemes are also depicted in the same figure and show that the dissipative nature of the scheme eliminates this problem. Note that the peak-to-peak value of the shear forces was 60 times larger for the EP scheme as compared with the ED scheme: clearly, the predictions of the EP schemes are completely obscured by numerical noise. The ED schemes eliminates these spurious oscillations and reveals the true peak-to-peak value of the shear forces. A similar behavior is observed for the mid-span bending moments. Note that the predictions of the EP scheme would be of little value in a design setting: indeed, it cannot predict stress levels to a reasonable level of accuracy.

This last example demonstrate that numerically dissipative schemes are necessary for dealing with physically stiff system. On the other hand, the previous examples have shown that constraints can be accurately enforced without resorting to numerical dissipation.

7. Conclusions

In present work, a new algorithm was developed for the enforcement of constraints within the framework of nonlinear, flexible multibody system modeled with the finite element approach. Constraints are

enforced through a Lagrange multiplier technique. The proposed algorithm exactly satisfies the constraints at the displacement and velocity levels, and furthermore, it achieves nonlinear unconditional stability by imposing the vanishing of the work done by the constraint forces. These three desirable features are intimately interrelated and stem from a specific discretization of the constraint Jacobian matrix whose existence is a direct consequence of the mean value theorem. Identical convergence rates are observed for the displacements, velocities, and Lagrange multipliers.

The algorithm accommodates scleronomic and rheonomic holonomic constraints, as well as non-holonomic constraints. Both EP and ED discretizations were presented for the constraint forces. It was shown that the proposed algorithm is closely related to the stabilized index-2 or GGL method. However, the proposed approach does not require additional Lagrange multipliers and does not rely on numerical dissipation for constraint stabilization. Unlike the classical GGL algorithm that enforces both position and velocity constraints at the final time, the present approach enforces the velocity constraint at the mid-point and the position constraint at the end point in time. This seems to suggest that imposing both position and velocity constraints at the same instant in time over-constrains the system.

The desirable characteristics of the algorithm for handling the constraints are obtained without resorting to numerically dissipative algorithms. If high frequencies are present in the system, i.e. the system is physically stiff, ED schemes are necessary to cope with the spurious high frequency oscillations observed when using EP algorithms.

Appendix A. Rodrigues parameters

A common representation of finite rotations (Kane and Levinson, 1985; Bauchau and Trainelli, in press) is in terms of Rodrigues parameters, $\underline{r} = 2\overline{n}\tan\phi/2$, where ϕ is the magnitude of the finite rotation and $\overline{n}$ the unit vector representing the axis of rotation. The finite rotation tensor R is expressed as

$$R(\underline{r}) = I + r_0\tilde{\overline{r}} + \frac{r_0}{2}\tilde{\overline{r}}\tilde{\overline{r}}, \tag{A.1}$$

where $r_0 = \cos^2\phi/2 = 1/[1 + (\overline{r}^{\mathrm{T}}\overline{r})/4]$. The following multiplicative decomposition of the rotation tensor is important

$$R = \left(I + \frac{1}{2}\tilde{\overline{r}}\right)\left(\frac{R+I}{2}\right), \tag{A.2}$$

and furthermore

$$I = \left(I - \frac{1}{2}\tilde{\overline{r}}\right)\left(\frac{R+I}{2}\right), \tag{A.3}$$

where I is the identity tensor.

References

Agrawal, O.P., Saigal, S., 1989. Dynamic analysis of multi-body systems using tangent coordinates. Computers and Structures 31, 349–355.

Amirouche, F.M.L., 1992. Computational Methods in Multibody Dynamics. Prentice-Hall, Englewood Cliffs, NJ.

Amirouche, F.M.L., Jia, T., Ider, S.K., 1988. A recursive householder transformation for complex dynamical systems with constraints. Journal of Applied Mechanics 55, 729–734.

Angeles, J., 1982. Spatial Kinematic Chains. Springer-Verlag, Berlin.

Bauchau, O.A., 1998. Computational schemes for flexible, nonlinear multi-body systems. Multibody System Dynamics 2, 169–225.

Bauchau, O.A., Bottasso, C.L., 1999. On the design of energy preserving and decaying schemes for flexible, nonlinear multi-body systems. Computer Methods in Applied Mechanics and Engineering 169, 61–79.

Bauchau, O.A., Theron, N.J., 1996. Energy decaying schemes for nonlinear elastic multi-body systems. Computers and Structures 59, 317–331.

Bauchau, O.A., Trainelli, L., in press. The vectorial parameterization of rotation. Nonlinear Dynamics.

Bauchau, O.A., Damilano, G., Theron, N.J., 1995. Numerical integration of nonlinear elastic multi-body systems. International Journal for Numerical Methods in Engineering 38, 2727–2751.

Bauchau, O.A., Choi, J.Y., Bottasso, C.L., 2002. Time integrators for shells in multibody dynamics. International Journal of Computers and Structures 80, 871–889.

Bauchau, O.A., Bottasso, C.L., Trainelli, L., 2003. Robust integration schemes for flexible multibody systems. Computer Methods in Applied Mechanics and Engineering 192, 395–420.

Baumgarte, J., 1972. Stabilization of constraints and integrals of motion in dynamic systems. Computer Methods in Applied Mechanics and Engineering 1, 1–16.

Bayo, E., Ledesma, R., 1996. Augmented Lagrangian and mass-orthogonal projection methods for constrained multibody dynamics. Nonlinear Dynamics 9, 113–130.

Bayo, E., Garcia de Jalon, J., Serna, M.A., 1988. A modified Lagrangian formulation for the dynamic analysis of constrained mechanical systems. Computer Methods in Applied Mechanics and Engineering 71, 183–195.

Borri, M., Croce, A., Trainelli, L., in press. The embedded projection method: A general index reduction procedure for constrained system dynamics. Computer and Mathematics with Applications.

Bottasso, C.L., Borri, M., 1997. Energy preserving/decaying schemes for non-linear beam dynamics using the helicoidal approximation. Computer Methods in Applied Mechanics and Engineering 143, 393–415.

Bottasso, C.L., Borri, M., Trainelli, L., 2001a. Integration of elastic multibody systems by invariant conserving/dissipating algorithms. Part I: formulation. Computer Methods in Applied Mechanics and Engineering 190, 3669–3699.

Bottasso, C.L., Borri, M., Trainelli, L., 2001b. Integration of elastic multibody systems by invariant conserving/dissipating algorithms. Part II: numerical schemes and applications. Computer Methods in Applied Mechanics and Engineering 190, 3701–3733.

Brenan, K.E., Campbell, S.L., Petzold, L.R., 1989. Numerical Solution of Initial-Value Problems in Differential-Algebraic Problems. North-Holland, New York.

Cardona, A., Géradin, M., 1989. Time integration of the equations of motion in mechanism analysis. Computers and Structures 33 (3), 801–820.

Chung, J., Hulbert, G.M., 1993. A time integration algorithm for structural dynamics with improved numerical dissipation: The generalized-α method. Journal of Applied Mechanics 60, 371–375.

Gear, C.W., 1988. Differential-algebraic equation index transformations. SIAM Journal on Scientific and Statistical Computing 9 (1), 40–47.

Gear, C.W., Petzold, L.R., 1984. ODE methods for the solution of differential/algebraic systems. SIAM Journal on Numerical Analysis 21 (4), 716–728.

Gear, C.W., Leimkuhler, B., Gupta, G.K., 1985. Automatic integration of Euler–Lagrange equations with constraints. Journal of Computational and Applied Mathematics 12, 77–90.

Géradin, M., Cardona, A., 2000. Flexible Multibody System: A Finite Element Approach. John Wiley & Sons, New York.

Hilber, H.M., Hughes, T.J.R., Taylor, R.L., 1977. Improved numerical dissipation for time integration algorithms in structural dynamics. Earthquake Engineering and Structural Dynamics 5, 282–292.

Hildebrand, F.B., 1976. Advanced Calculus for Applications, second ed. Prentice Hall, Englewood Cliffs, NJ.

Kane, T.R., Levinson, D.A., 1985. Dynamics: Theory and Applications. McGraw-Hill, New York.

Kim, S.S., Vanderploeg, M.J., 1986. QR decomposition for state space representation of constrained mechanical dynamic systems. Journal of Mechanisms, Transmissions and Automation in Design 108, 183–188.

Kurdila, A., Papastavridis, J.G., Kamat, M.P., 1990. Role of Maggi's equations in computational methods for constrained multibody systems. Journal of Guidance, Control, and Dynamics 13 (1), 113–120.

Liang, C.G., Lance, G.M., 1987. A differentiable null space method for constrained dynamic analysis. Journal of Mechanisms, Transmissions and Automation in Design 109, 405–411.

Lotstedt, P., Petzold, L.R., 1986a. Numerical solution of nonlinear differential equations with algebraic constraints I: Convergence results for backward differentiation formulas. Mathematics of Computation 46, 491–516.

Lotstedt, P., Petzold, L.R., 1986b. Numerical solution of nonlinear differential equations with algebraic constraints II: Practical implications. SIAM Journal on Scientific and Statistical Computing 7, 720–733.

Mani, N.K., Haug, E.J., Atkinson, K.E., 1985. Application of the singular value decomposition for analysis of mechanical system dynamics. Journal of Mechanisms, Transmission, and Automation in Design 107, 82–87.

Newmark, N.M., 1959. A method of computation for structural dynamics. Journal of the Engineering Mechanics Division 85, 67–94.

Nikravesh, P.E., 1988. Computer-Aided Analysis of Mechanical Systems. Prentice-Hall, Englewood Cliffs, NJ.

Orlandea, N., Chace, M.A., Calahan, D.A., 1977. A sparsity oriented approach to the dynamic analysis and design of mechanical systems. Parts I and II. ASME Journal of Engineering for Industry 99 (3), 773–784.

Papastavridis, J.G., 1990. Maggi's equations of motion and the determination of constraint reactions. Journal of Guidance, Control, and Dynamics 13 (2), 213–220.

Park, K.C., Chiou, J.C., 1988. Stabilization of computational procedures for constrained dynamical systems. Journal of Guidance, Control, and Dynamics 11 (4), 365–370.

Park, K.C., Chiou, J.C., Downer, J.D., 1988. Explicit-implicit staggered procedure for multibody dynamics analysis. Journal of Guidance, Control, and Dynamics 13 (3), 562–570.

Puso, M.A., 2002. An energy and momentum conserving method for rigid–flexible body dynamics. International Journal for Numerical Methods in Engineering 53, 1393–1414.

Schiehlen, W.O. (Ed.), 1990. Multibody System Handbook. Springer-Verlag, Berlin.

Simo, J.C., Tarnow, N., 1992. The discrete energy-momentum method. Conserving algorithms for nonlinear dynamics. ZAMP 43, 757–792.

Simo, J.C., Tarnow, N., 1994. A new energy and momentum conserving algorithm for the nonlinear dynamics of shells. International Journal for Numerical Methods in Engineering 37, 2527–2549.

Simo, J.C., Wong, K., 1991. Unconditionally stable algorithms for rigid body dynamics that exactly preserve energy and momentum. International Journal for Numerical Methods in Engineering 31, 19–52.

Simo, J.C., Tarnow, N., Doblare, M., 1995. Non-linear dynamics of three-dimensional rods: Exact energy and momentum conserving algorithms. International Journal for Numerical Methods in Engineering 38, 1431–1473.

Singh, R.P., Likins, P.W., 1985. Singular value decomposition for constrained dynamical systems. Journal of Applied Mechanics 52, 943–948.

Stol, K., Bir, G., Balas, M., 1999. Linearized dynamics and operating modes of a simple wind turbine model. In: Proceedings of the 37th AIAA Aerospace Sciences Meeting and Exhibit. 11–14 January, Reno, Nevada, pp. 135–142, NICH Report No. 32548.

Walton, W.C., Steeves, E.C., 1969. A new matrix theorem and its application for establishing independent coordinates for complex dynamical systems with constraints. Technical Report NASA TR R-326, NASA.

Wehage, R.A., Haug, E.J., 1982. Generalized coordinate partitioning for dimension reduction in analysis of constrained dynamic systems. ASME Journal of Mechanical Design 104, 247–255.